Springer

Journal of
Mechanical
Science and
Technology

Journal of Mechanical Science and Technology 22 (2008) 2445~2453

www.springerlink.com/content/1738-494x
DOI 10.1007/s12206-008-0907-6

Robust motion control of a clamp-cylinder for energy-saving injection moulding machines †

Seung Ho Cho[1,*] and Siegfried Helduser[2]

[1]*Department of Mechanical and System Design Engineering, Hongik University, Seoul, 121-791, Korea*
[2]*Institute of Fluid Power and Motion Control, Technical Universität Dresden, Germany*

(Manuscript Received May 19, 2008; Revised September 6, 2008; Accepted September 9, 2008)

Abstract

This paper deals with the issue of robust motion control of a clamp-cylinder for injection moulding machines driven by a pair of speed-controlled fixed displacement pumps. As a fundamental step prior to tracking controller design, a feedback control system is suggested by implementing a position control loop in parallel with a system pressure control loop. A discrete-time sliding mode control scheme is developed for enhancing the tracking performance under inherent nonlinearities. Consequently, a significant reduction in tracking error is achieved for both position and pressure control applications.

Keywords: Robust motion control; Speed-controlled fixed displacement pump; Injection moulding machines; Clamp-cylinder; Sliding mode controller

1. Introduction

Energy-saving issues in injection moulding machines [1-5] have brought forth direct pump control as an efficient way to drive a clamp-cylinder by replacing the directional control valve. Also, users of new energy-saving hydraulic drives may be strongly interested in the basic features of the overall system as well as operating efficiency or noise characteristics. The overall system includes a hydraulic pump, cylinder, and control electronics. Therefore, besides the research of components in itself, the development and research of an appropriate cylinder circuit is basically important for broadly utilized energy-saving hydraulic drive systems [6, 7]. Direct pump control of a differential cylinder-load system is preferred due to its convenience in view of system assembling process and its capability of generating high force in extending motion. However, it is necessary to compensate for the different volumetric flow rate due to piston area ratio. In this paper, a pair of speed-controlled fixed displacement pumps are utilized to drive a differential cylinder for clamping. Prior to tracking controller design, mathematical modeling and analysis of the overall system is performed. The clamp-cylinder for injection moulding may be required to perform under a variety of operating conditions; therefore robust control performance is important, particularly in trajectory tracking control applications. Recently, one of the authors of this paper presented a sliding mode tracking control scheme in combination with a nonlinear friction compensator [8]. This paper intends to show how the injection-moulding clamp-cylinder drives, consisting of AC servomotor, speed-controlled fixed displacement pump, differential cylinder, toggle clamp system, behave under the sliding mode tracking control scheme. A sliding mode controller combining feedback control scheme with velocity feedforward is developed for compensation of inherent nonlinearities and modeling error. Section 2 shows an over-

† This paper was recommended for publication in revised form by Associate Editor Dong Hwan Kim

*Corresponding author. Tel.: +82 2 320 1682, Fax.: +82 2 322 7003
E-mail address: shcho@wow.hongik.ac.kr

view of feedback control structure with electric-hydrostatic system. Section 3 describes mathematical modeling and analysis for a clamp-cylinder drive system with its operating principles. Section 4 describes the design process of sliding mode tracking controller combining feedback control scheme with velocity feedforward. Section 5 describes computer simulation results, and Section 6 concludes.

2. Feedback control of electric-hydrostatic system

The electric–hydrostatic system around a toggle-operated clamp is shown in Fig. 1. The differential cylinder is driven by a pair of speed-controlled fixed displacement pumps, which are combined with AC servomotors independently. With reference to model in Fig. 1, the maximum clamping force is 1200kN. The main advantage of this drive scheme lies in the insensitivity of cylinder velocity to load pressure change, in addition to the capability of load pressure amplification according to pump revolution number.

Fig. 2 shows the feedback control structure based on Fig. 1 for a clamp-cylinder in a plastics injection moulding machine, which operates on the principle of rapid extension. Cylinder velocity and acceleration is controlled by pump 2, and the flow rate difference induced by the piston area characteristics of differential cylinder is compensated by pump 1. During extending motion, pump 1 delivers oil to the cylinder chamber and during retracting motion, the excess flow rate returns to tank. While two pumps operate approximately under the same revolution, the flexibility of this control method is enhanced by two independent control variables n_1, n_2. Both chambers of the cylinder maintain a desired state without additional hydraulic components, which is accomplished by employing an appropriate control method. For the purpose of overall system control, both the position controller and pressure controller are used simultaneously. While the cylinder is operating, the sum pressure, i.e., the sum of pressures in both chambers, is controlled. Output values of pressure and position controller are added and then they are used to drive both pumps. In this control structure, the change of leakage value, which depe-

nds on temperature and wear condition, may be compensated in itself. Piston balance may be accomplished by increasing the system pressure level during working cycle, and thus the dynamic charac-

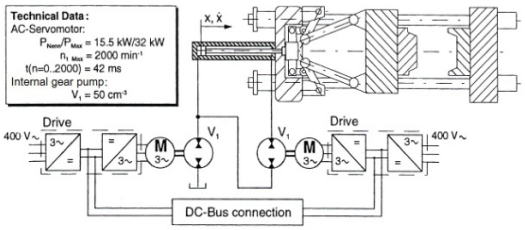

Fig. 1. Schematic of electric-hydrostatic system around a toggle-operated clamp.

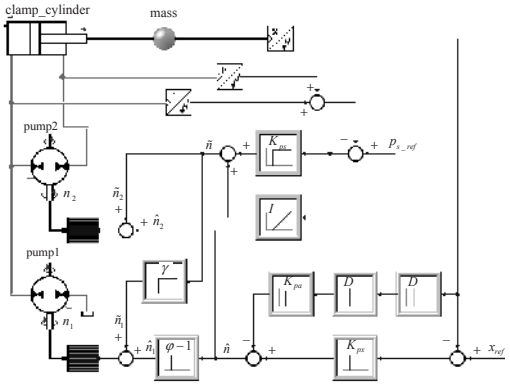

Fig. 2. Feedback control structure for clamp-cylinder drives

teristics of the driving system are enhanced to essentially improve the control performance.

Under the control method described above, the driving system operates similarly as a valve-controlled system. The pressure control system maintains the sum pressure constant under the additional load increase or during the acceleration mode of the piston.

During these periods the absolute value of each pressure in both chambers changes in the opposite direction, and thus the balance of the external load is maintained or the piston rod is accelerated. Based on these advantageous features, the analysis of position control is to be performed under system pressure control.

3. Modeling and analysis of pump-cylinder clamping unit

As a subsystem of the electric–hydrostatic system in Fig. 2, the pump-cylinder drives with parameters are shown in Fig. 3. The number of revolutions of both pumps is derived by using piston area characteristics $\varphi = A_A / A_B$ and leakage factor γ, assuming that volumetric displacements are

equal: $V_1 = V_2$. The leakage factor shows a relationship between the number of revolutions of both pumps in accordance with leakage characteristics of the overall system.

$$\hat{n}_1 = (\varphi - 1)\ \hat{n}_2 \tag{1}$$

$$\tilde{n}_1 = \gamma \cdot \tilde{n}_2 \tag{2}$$

The piston area characteristics as well as the leakage factor are concerned with control parameters of the position and pressure control system described in Fig. 2 of Section 2. The leakage factor is obtained under active pressure control, and it is derived by adjusting the revolution characteristics of the pump to leakage behavior under no load condition. This enables avoiding cylinder drift, for which the position control system needs to compensate. Eventually, the accuracy of this drive system is enhanced. The command for revolution number of each pump, i.e. , $n_{i(i=1,2)}$ is composed of control values $\hat{n}_{i(i=1,2)}$ and $\tilde{n}_{i(i=1,2)}$, which are derived from the position control system and pressure control system, respectively.

$$n_1 = \hat{n}_1 + \tilde{n}_1, \quad n_2 = \hat{n}_2 + \tilde{n}_2 \tag{3}$$

To describe the static and dynamic characteristics, the parameters shown in Fig. 3 are used, in which the following equations hold.

$$p_s = p_A + p_B \tag{4}$$

$$p_L = \varphi \cdot p_A - p_B \tag{5}$$

The leakage factor γ is derived from the continuity equation of cylinder chambers A and B under no load condition $p_L = 0$ and piston velocity $\dot{x} = 0$.

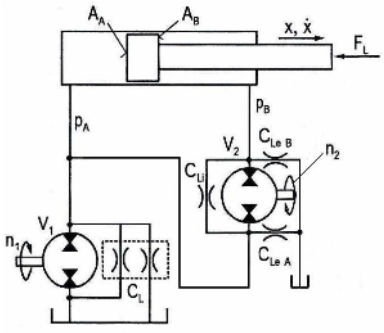

Fig. 3. Parameters of pump-cylinder drives.

$$\tilde{n}_1 V_1 + C_{Li}(p_B - p_A) = (C_L + C_{LeA})p_A + \tilde{n}_2 V_1 \tag{6}$$

$$\tilde{n}_2 V_1 = C_{Li}(p_A - p_B) + C_{LeB} p_B \tag{7}$$

From the definition of sum pressure p_S , the pressure p_A , p_B becomes.

$$p_A = \frac{p_S + p_L}{\varphi + 1}, \quad p_B = \frac{\varphi p_S - p_L}{\varphi + 1} \tag{8}$$

By letting $p_L = 0$ in Eqs. (6) and (7) and then applying equation (8), the expression for pump revolution is obtained as follows.

$$\tilde{n}_1 = \frac{p_S}{V_1}\left[\frac{1}{\varphi + 1}(C_L + C_{LeA}) + \frac{\varphi}{\varphi + 1} C_{LeB}\right] \tag{9}$$

$$\tilde{n}_2 = \frac{p_S}{V_1}\left[\frac{\varphi - 1}{\varphi + 1} C_{Li} + \frac{\varphi}{\varphi + 1} C_{LeB}\right] \tag{10}$$

The leakage factor γ is obtained from equations (9) and (10).

$$\gamma = \frac{\tilde{n}_1}{\tilde{n}_2} = \frac{C_L + C_{LeA} + \varphi C_{LeB}}{(\varphi - 1)C_{Li} + \varphi C_{LeB}} \tag{11}$$

In the clamp-cylinder drive system shown in Fig. 2, the output variables consist of cylinder position x and pressure p_S. In practical applications, the system pressure normally reaches the desired reference value before the position controller begins to work. While the pressures p_A and p_B change in opposite directions, maintaining the pressure difference required, the sum pressure is always constant. Therefore, the position control circuit may be considered alone. Oil columns in both chambers are regarded as oil spring for clamping.

The following differential equations are employed to describe dynamic characteristics:

Newton's equation of motion:

$$A_B \cdot P_L = m_{eq} \cdot \ddot{x} + b \cdot \dot{x} + F_L \tag{12}$$

Pressure build-up equation in cylinder volume V_A and V_B:

$$\frac{dp_A}{dt} = \frac{K_{oilA}}{V_A}[\hat{n}_1 V_1 + \hat{n}_2 V_1 - \dot{x} A_A + (p_B - p_A)C_{Li} - p_A(C_L + C_{LeA})] \tag{13}$$

$$\frac{dp_B}{dt} = \frac{K_{oilB}}{V_B}\left[\dot{x}A_B - \hat{n}_2 V_1 - (p_B - p_A)C_{Li} - C_{LeB}p_B\right] \quad (14)$$

From Eqs. (13) and (14), the build-up equation for load pressure yields.

$$\frac{dp_L}{dt} = \varphi\frac{dp_A}{dt} - \frac{dp_B}{dt} \quad (15)$$

In the process of substituting Eqs. (1), (8), (13) and (14), the leakage due to system pressure p_S and the volume flow required to maintain equilibrium, i.e., $\tilde{n}_1 V_1$, $\tilde{n}_2 V_1$ are not considered.

$$\frac{dp_L}{dt} = \frac{K_{oil}}{V_B}\left[(\varphi+1)\hat{n}_2 V_1 - (\varphi+1)\dot{x}A_B - p_L\left(\frac{C_L + C_{LeA} + C_{LeB} - 4C_{Li}}{\varphi+1}\right)\right] \quad (16)$$

The equivalent leakage coefficient depending on system load pressure is expressed as follows.

$$C_{Leq} = \frac{C_L + C_{LeA} + C_{LeB} - 4C_{Li}}{\varphi+1} \quad (17)$$

As a result of linearization, a simplified block diagram of electric-hydrostatic cylinder drives with speed-controlled hydraulic pump is shown in Fig. 4. This differential cylinder is considered as a 2nd-order system with a free integrator. By comparing the coefficient with a standard 2nd-order system, the natural frequency and damping ratio of hydraulic control system is derived.

$$\omega_h = \sqrt{\frac{K_{oil}\left[bC_{Leq} + (\varphi+1)A_B^2\right]}{V_B m_{eq}}} \quad (18)$$

$$D_h = \frac{m_{eq}K_{oil}C_{Leq} + bV_B}{2K_{oil}\left[bC_{Leq} + (\varphi+1)A_B^2\right]\sqrt{\frac{K_{oil}\left[bC_{Leq} + (\varphi+1)A_B^2\right]}{V_B m_{eq}}}} \quad (19)$$

$$K_V = \frac{A_B K_{AC} V_1(\varphi+1)}{bC_{Leq} + (\varphi+1)A_B^2} \quad (20)$$

From the block diagram in Fig. 4, we notice that electric-hydrostatic differential cylinder drives principally exhibit the same control structure as a valve-controlled system. To enhance the static and dynamic

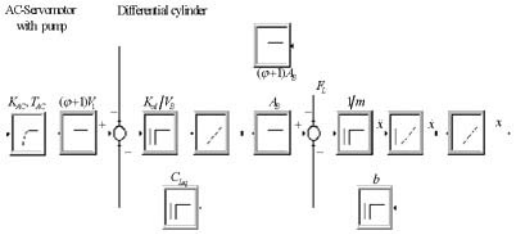

Fig. 4. Open-loop configuration under system pressure control.

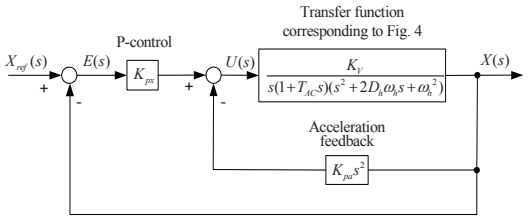

Fig. 5. Closed-loop configuration.

characteristics of the system in Fig. 4, a feedback control system is constructed as shown in Fig. 5 by installing a position controller with acceleration feedback. To investigate the open loop characteristics, computer simulations are performed for the circuit composed of AC servomotor, pump, differential cylinder, and toggle-operated clamp. Prior to analysis of the open loop response, the natural frequency of differential cylinder in combination with toggle-operated clamp was examined via the process of deriving its equivalent mass load on piston rod. Figure 6 shows the behavior of natural frequency and equivalent mass m_{eq} according to cylinder displacement. We notice that the mechanism of toggle-operated clamp influences the design parameters. Fig. 7 demonstrates the simulation results of open loop response for a range of input voltage. The simulation model is composed of AC servomotor, pump, differential cylinder, and toggle-operated clamp. In the simulation model, the dynamics of the AC servomotor has been considered as a first-order system with time constant T_{AC} = 0.002 second and motor constant K_{AC} = 2.58. The transient response in velocity waveform shows an underdamped oscillatory motion with damping ratio D_h = 0.21 and natural frequency ω_h = 84.8 rad/s (=13.5 Hz). Considering the dynamics of the AC servomotor, it may be approximated to a 2nd-order linear model. Referring to Fig. 7, when the input is 0.020 volt, the displacement shows a saturation phenomenon due to a stop at the end of stroke, and correspondingly the velocity waveform suddenly drops to zero.

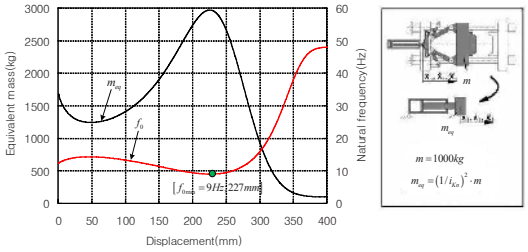

Fig. 6. Natural frequency and equivalent mass.

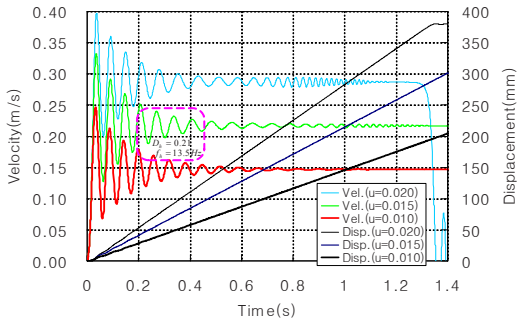

Fig. 7. Open loop responses of simulation model.

4. Feedforward tracking control schemes

In the design and analysis of physical systems, the continuous-time approach is known to be effective for modeling the inherent characteristics and describing the design parameters. On the other hand, a one-chip microcontroller is often utilized for industrial applications, which has motivated the design of a discrete-time controller for injection moulding clamp-cylinder drives.

To enhance the tracking control performance, a discrete-time sliding mode controller combined with feedback control schemes is suggested.

The z-transform with zero-order hold for the minor loop in Fig. 5 yields

$$Z\left\{\frac{1-e^{-Ts}}{s}\cdot\frac{K_V}{s\left[(1+T_{AC}s)(s^2+2D_h\omega_h s+\omega_h{}^2)+K_V K_{pa}s\right]}\right\}$$

$$=(1-z^{-1})Z\left\{\frac{K_V}{s^2\left[(1+T_{AC}s)(s^2+2D_h\omega_h s+\omega_h{}^2)+K_V K_{pa}s\right]}\right\} \quad (21a)$$

$$=\frac{z^{-1}(b_0+b_1z^{-1}+b_2z^{-2}+b_3z^{-3})}{1+a_1z^{-1}+a_2z^{-2}+a_3z^{-3}+a_4z^{-4}} \quad (21b)$$

$$=\frac{z^{-1}B(z^{-1})}{A(z^{-1})} \quad (21c)$$

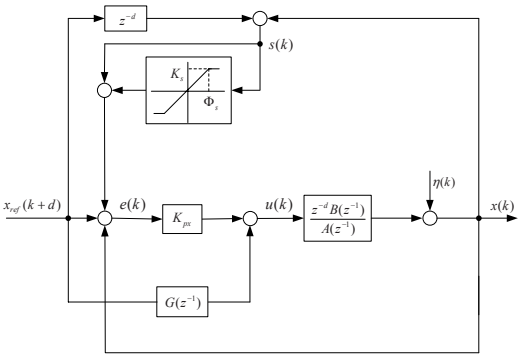

Fig. 8. Block diagram for sliding mode control.

The coefficients, $a_{i(i=1\sim4)}$ and $b_{i(i=0\sim3)}$ are functions of K_{pa}, K_V, T_{AC}, D_h, and ω_h. It may be expressed in general input-output form as follows:

$$x(k)=\frac{z^{-d}B(z^{-1})}{A(z^{-1})}u(k)+\eta(k)\,. \quad (22)$$

In Eq. (22), $u(k)$ and $x(k)$ are the measurable input and output, respectively, and $\eta(k)$ represents a modeling error. In this paper, in order to compensate for the inherent nonlinearities and to achieve robust tracking control, a discrete-time sliding mode tracking control scheme is adopted. The control scheme combines feedback control with a discrete time version of sliding mode control. The block diagram for the design of discrete-time sliding mode controller is shown in Fig. 8.

If there exists no modeling error, i.e., $\eta(k)=0$, the control law for perfect tracking can be obtained by letting the tracking error satisfy

$$x(k+d)-x_{ref}(k+d)=0\,. \quad (23)$$

From Eqs. (22) and (23), the control error signal becomes under velocity feedforward.

$$e(k)=\frac{1}{K_{px}}\cdot\left[\frac{A(z^{-1})}{B(z^{-1})}\cdot x_{ref}(k+d)-G(z^{-1})\cdot x_{ref}(k+d)\right] \quad (24)$$

Where the transfer function for velocity feedforward is as follows

$$G(z^{-1})=z^{-d}\cdot K_{vf}\cdot\frac{1}{T}(1-z^{-1})\,.$$

However, with $\eta(k) \neq 0$ the requirement set by Eq. (23) cannot be achieved by using the control law given by Eq. (24). To compensate for modeling error a sliding surface is introduced, as defined by Eq. (25).

$$s(k) = x(k) - x_{ref}(k) . \tag{25}$$

Both outside and inside the boundary layer, the control law given by Eq. (24) is now modified to become

$$e(k) = \frac{1}{K_{px}} \cdot \left\{ \frac{A(z^{-1})}{B(z^{-1})} \cdot \left[s(k) + x_{ref}(k+d) - K_s sat\left(\frac{s(k)}{\Phi_s} \right) \right] - G(z^{-1}) \cdot x_{ref}(k+d) \right\} \tag{26}$$

Where

$$\text{sat}\left(\frac{s(k)}{\Phi_s} \right) = \begin{cases} +1 & \text{for} \quad \Phi_s \le s(k) \\ \dfrac{s(k)}{\Phi_s} & \text{for} \quad -\Phi_s < s(k) < \Phi_s \\ -1 & \text{for} \quad s(k) \le -\Phi_s \end{cases}$$

Notice that from Eqs. (25) and (26), the sliding function $s(k)$ satisfies,

$$s(k+d) = s(k) - K_s sat\left(\frac{s(k)}{\Phi_s} \right) + \eta(k+d) . \tag{27}$$

Inside the sliding boundary layer, the s-dynamics become:

$$s(k+d) = \left(1 - \frac{K_s}{\Phi_s} \right) s(k) + \eta(k+d) \tag{28}$$

Eq. (28) shows a first-order filter with input $\eta(k+d)$ and eigenvalue λ

$$1 - \frac{K_s}{\Phi_s} = \lambda . \tag{29}$$

The parameter Φ_s determines the size of the boundary layer around $s(k) = 0$. The boundary layer provides robustness against modeling error. The modeling error which ultimately affects the tracking performance is diluted in the sliding boundary layer by way of saturation function, which results in robustness increase. Proof of the convergence of this scheme and a discussion on the selection of K_s and Φ_s is given by Cho [9]. The control methods adopted are listed in Table 1. Sliding mode control is applied to position and pressure control loop, respectively.

Table 1. Control method classification.

	P-control	Velocity feedforward	Position - sliding mode	Pressure sliding mode
Control 1	O			
Control 2	O	O		
Control 3a	O	O	O	
Control 3b	O	O	O	O

5. Computer simulation and discussions

Computer simulations are performed according to control methods described in Table 1. Component parameters and controller parameters for simulation are shown in Table 2 and Table 3, respectively. The gain in P-controller has been determined from simulation of step responses. The maximum gain in P-controller that does not yield an oscillatory motion has been adopted. The velocity feedforward gain has been derived, based on open loop gain which has been formulated algebraically to be unity. Eighty percent weighting to the normalized open loop gain, i.e., 0.8 has been chosen finally for velocity feedforward gain considering tracking performance. The parameters in sliding mode controller are determined by using equation (29) based on eigenvalue $\lambda = 0.5$. Boundary layer width is provided to avoid chattering. As an external load for simulation of clamp-cylinder drives, a 3D toggle system has been constructed through multibody dynamics module in ITI SimulationX. Reference trajectories are generated according to the process in the motion of the mold as shown in Fig. 9. In order to investigate the trajectory tracking performance under different modes, the reference trajectory is formulated by combining acceleration mode, constant speed mode, deceleration mode and stopping mode. The reference displacement is used for command input signal in trajectory tracking control. It is required to achieve position tracking error near zero at the final stage of clamping force

build-up process to prevent burr formation, and also it is needed to achieve pressure tracking error within 10% of the reference system pressure for high quality products. In simulation, the information of load pressure is utilized for obtaining acceleration. Simulation results of three control schemes, i.e., control 1, control 2, and control 3a, are shown in Fig. 10. From Fig. 10 we may notice that velocity feedforward control speeds up the response to a certain degree. However, it does not reach a perfect tracking. By combining a sliding mode scheme in position control loop, a significant reduction in tracking error is achieved. Especially during the period from 0.58 second to 0.60 second, which corresponds to the final process of clamping force build-up and is also important for preventing burr formation, the tracking error reaches near zero by a position sliding mode control. Next, sliding mode control is applied to the position control loop and system pressure control loop simultaneously. The corresponding simulation results are shown in Fig. 11, where the reference system pressure is constant at 240bar. From Fig. 11, we notice that control 3a and control 3b show the same tendency in view of position tracking control. However, in view of pressure tracking control, control 3b shows a far better response than control 3a.

Table 2. Component parameters for simulation.

Parameters		value
Cylinder	Piston diameter	90 mm
	Rod diameter	65 mm
Pump	Volumetric displacement $V_1(=V_2)$	50 cm^3
	Volumetric efficiency	90 %
	Mechanical efficiency	90 %

Table 3. Controller parameters for simulation.

P-control	Velocity feedforward	Position-sliding mode	Pressure-sliding mode
$K_{px} = 18$	$K_{vf} = 0.8$	$K_s = 5$ $\Phi_s = 10$	$K_s = 3.5$ $\Phi_s = 7$

Fig. 12 shows the angular velocity of the AC servomotor and cylinder chamber pressure under control 3b. The motor starts according to the reference desired trajectory in Fig. 9. So a slope at transient response may be expected with its dynamics considered. During most of the simulation, the pressures p_A and p_B change in opposite directions according to load. Due to the inherent characteristics of maintaining the system pressure, i.e., sum pressure constant, both cylinder capacities are pressurized and operate as active oil-spring, through which a high dynamic is achieved. It is remarkable that a differential cylinder driven by electric-hydrostatic system shows characteristics of a valve-controlled

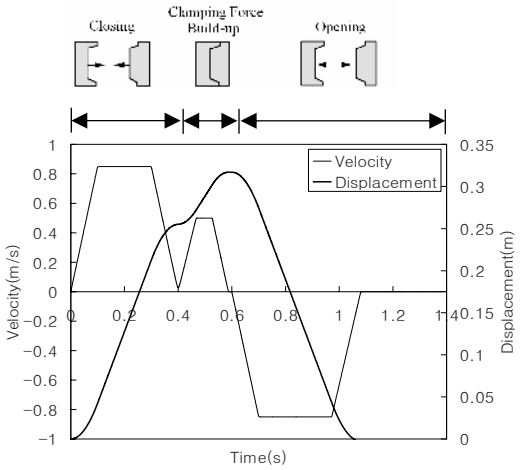

Fig. 9. Reference trajectory for cylinder rod.

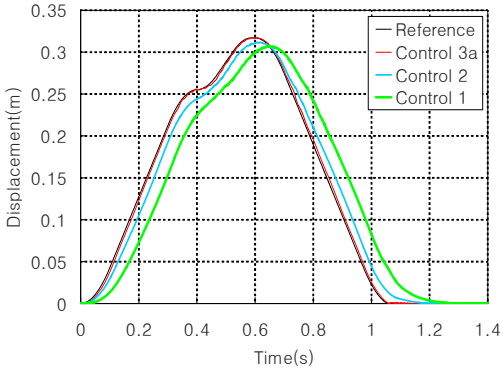

Fig. 10. Comparison of output trajectories.

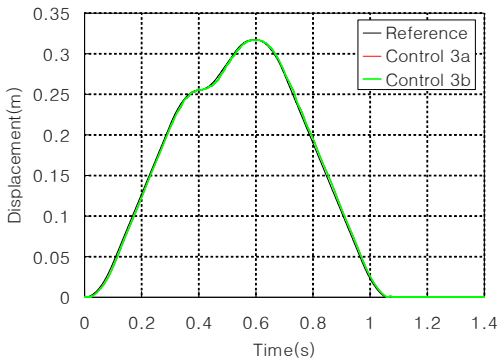

(a) Position tracking performance

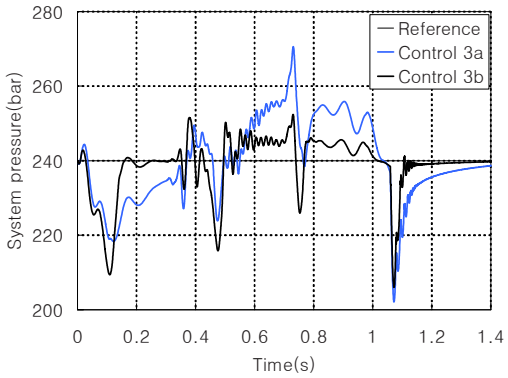

(b) Pressure tracking performance

Fig. 11. Comparison of sliding mode controls.

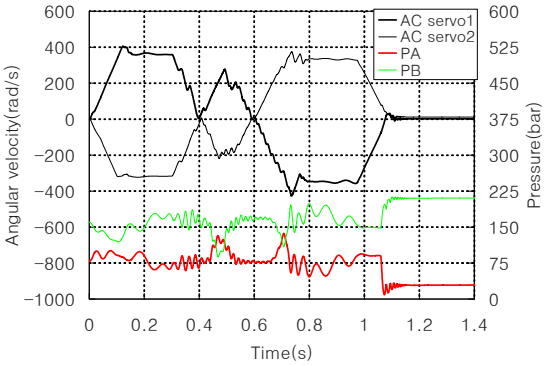

Fig. 12. AC servomotor velocity and chamber pressure (control 3b).

system. The function of a system pressure control, i.e., the coupling of both pump revolution numbers corresponds to a mechanical coupling of control edge in a valve. Fig. 13 shows the behavior of clamping force build-up processes. When a sliding-mode control scheme is applied, the clamping force takes the form of tooth-like shape favorable for clamping and also

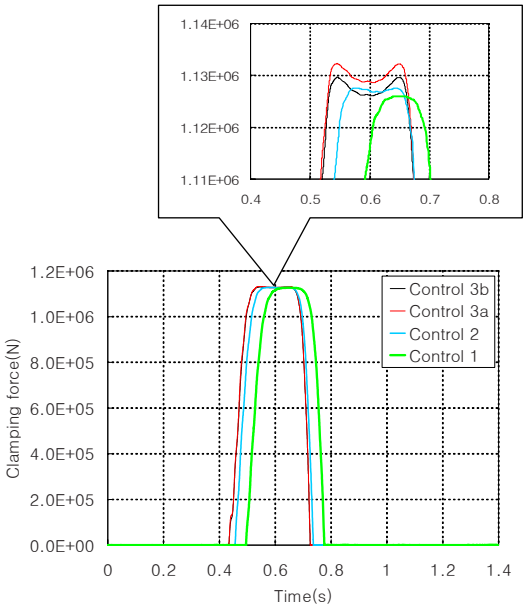

Fig. 13. Comparison of clamping force build-up processes.

the magnitude of clamping force increases. We are now preparing experiments to validate computer simulation and the result will appear in the near future.

6. Conclusions

Mathematical modeling and analysis are performed for a clamp-cylinder of injection moulding machines driven by a pair of speed-controlled fixed displacement pumps. A feedback control system has been constructed for a position control loop and pressure control loop, respectively. A sliding mode tracking controller is designed in combination with a velocity feedforward loop for enhancing tracking performance. Control performance is compared in view of position and pressure tracking by means of computer simulation. When sliding mode control has been applied to position control loop, position tracking error has been decreased markedly. When sliding mode control has been applied to both position and pressure control loop, significant reduction in pressure tracking error has been achieved especially where the position tracking error remains almost the same. Simulation results show that a differential cylinder driven by AC servomotor-hydraulic pump shows characteristics of a valve-controlled system. It is also shown that sliding mode control may be utilized efficiently for clamping force build-up.

Acknowledgment

This work was supported by the Korea Research Foundation Grant funded by the Korean Government(KRF-2007-614-D00012).

References

[1] S. Helduser, Development Trends in Electrohydraulic Drives and Controls, 6th Internationales Fluidtechnisches Kolloquium, Dresden 2008, Germany, (2008) 29-64.

[2] S. Helduser, Electric-hydrostatic drive systems and their application in injection moulding machines, The Fourth JHPS International Symposium on Fluid Power, November 12-15, Yokohama, Japan, (1999) 261-266.

[3] S. Helduser and Th. Neubert, Improved Energy Efficiency in Plastic Injection Moulding Machines, 8th Scandinavian International Conference on Fluid Power, SICFP'03, Tampere, Finland.

[4] J. Wortberg, Th. Kamps, and R. Schiffers, Welches Energie kostet ein Antrieb?, Kunststoffe 93(6), 2003, 62-69.

[5] T. Rober, Analyse des Betriebsverhaltens von vollelektrischen gegenueber hydrualisch angetriebenen Spritzgieβmaschinen basierend auf Vergleichsmessungen, Dissertation, RWTH Aachen, 1995.

[6] A. Helbig, Injection Moulding Machine with Electric-Hydrostatic Drives, 3rd Internationales Fluidtechnisches Kolloquium, Aachen 2002, Germany, 2002, 67-81.

[7] Q. Long and Th. Neubert, Hochdynamische Lageregelung fuer Differenzialzylinder mit zwei drehzahlgeregelten Pumpen, hydraulik und Pneumatik 44, Nr. 9, 2000.

[8] S. H. Cho and K. A. Edge, Adaptive sliding mode tracking control of hydraulic servosystems with unknown nonlinear friction and modelling error. Proc. Inst. Mech. Engrs., Part I, Journal of Systems and Control Engineering, 2000, 214(4), 247-257.

[9] S. H. Cho, Robust discrete time tracking control using sliding surfaces. KSME Int. J., 1995, 9 (1), 80-90.

Notation

A_A , A_B : Piston areas of head side and rod side
C_L , C_{Li} : Total leakage coefficient and internal leakage coefficient
C_{LeA}, C_{LeB} : External leakage coefficients at connections A and B
K_{px} K_{pa} : Proportional gain of position controller and acceleration feedback gain
K_{ps} : Proportional gain of pressure controller
K_s, K_{vf} : Sliding mode controller gain and velocity feedforward gain
V_1 , V_2 : Volumetric displacements of pump 1 and pump 2
V_A, V_B : Volumes of cylinder chamber A and B

Seung Ho Cho received his B.S., M.S., and Ph.D. degrees from Seoul National University in 1978, 1981, and 1986, respectively. He then went on to perform his Post-Doc. research from U.C. Berkeley in 1989-1990. Dr. Cho is currently a Professor at the Mechanical and System Design Engineering of Hongik University in Seoul, Korea. Dr. Cho's research interests are in the area of automatic control applications, fluid power control, and energy-saving drive systems.